Optimal Gating Window for Respiratory-Gated Pencil Beam Scanning Proton Therapy for Lung Cancer: A pilot study

ขนาดของช่วงการฉายรังสีต่อรอบการหายใจที่เหมาะสมสำหรับการฉายอนุภาคโปรตอนด้วยเทคนิคการสแกนลำรังสีขนาดเล็กตามจังหวะการหายใจเพื่อการรักษาโรคมะเร็งปอด: การศึกษานำร่อง

Nattakarn Kittiva[1], Thiansin Liamsuwan[1], Chirasak Khamfongkhruea[2], Sasikarn Chamchod[1,2] Sumana Paduka[2]

[1]Faculty of Medicine and Public Health, HRH Princess Chulabhorn College of Medical Science, Chulabhorn Royal Academy, Bangkok, Thailand

[2]Department of Radiation Oncology, Chulabhorn Hospital, Bangkok, Thailand

Corresponding author

Thiansin Liamsuwan

Faculty of Medicine and Public Health, HRH Princess Chulabhorn College of Medical Science, Chulabhorn Royal Academy, Bangkok, Thailand

906 Kamphaeng Phet 6 Rd., Talat Bang Khen, Lak Si, Bangkok 10210, Thailand

Email: thiansin.lia@pccms.ac.th

ณัฐกานต์ กิจทิวา[1], เธียรสิน เลี่ยมสุวรรณ[1], จีรศักดิ์ คำฟองเครือ[1], ศศิกาญจน์ จำจด[1,2] สุมนา ปะดุกา[2]

[1]คณะแพทยศาสตร์และการสาธารณสุข วิทยาลัยวิทยาศาสตร์การแพทย์เจ้าฟ้าจุฬาภรณ์ ราชวิทยาลัยจุฬาภรณ์

[2]งานรังสีรักษาและมะเร็งวิทยา โรงพยาบาลจุฬาภรณ์

ผู้นิพนธ์ประสานงาน

เธียรสิน เลี่ยมสุวรรณ

คณะแพทยศาสตร์และการสาธารณสุข วิทยาลัยวิทยาศาสตร์การแพทย์เจ้าฟ้าจุฬาภรณ์ ราชวิทยาลัยจุฬาภรณ์

906 ถ.กำแพงเพชร 6 แขวงตลาดบางเขน เขตหลักสี่ กทม. 10210

อีเมล: thiansin.lia@pccms.ac.th

Submitted: May 28, 2021

Revised: July 24, 2021

Accepted: August 4, 2021

Abstract

Backgrounds: Pencil beam scanning (PBS) proton therapy has the capability of delivering conformal dose to the target with a relatively low dose to normal tissues. Several studies have shown the advantages of PBS for lung cancer treatment. However, respiratory motion causes the interplay effect between organ motion and dynamic beam delivery.

Objective: To investigate the efficiency of gated PBS proton therapy for a lung cancer patient with the target motion of larger than 10 mm for different gating windows (GWs) by considering dosimetric parameters of organs at risk (OARs) and treatment time.

Materials and Methods: The four-dimensional computed tomography (4DCT) dataset of a lung cancer patient with the target motion of 11.6 mm was used in this study. The internal target motion was defined by deformable image registration of the GTV in each respiratory phase to end-exhalation phase, while the external motion was defined by using the RPMTM (Real-time-Position-Management) data. The relationship between external and internal motion was investigated. The treatment plans for the different GWs with internal motion ranging from 2 mm to 11.6 mm were created using matRad, an open-source treatment planning system for generic treatment machines. The dosimetric parameters for OARs from each plan were compared using the ungated plan as the reference. The treatment time was evaluated based on published data of Varian's ProBeam.

Results: The treatment plans with the GWs of 10%-80%, 20%-70%, 30%-70% and 40%-60% resulted in the reduction of Dmean in the heart by 1.43-14.29% and the reduction of Dmean in the lung by 2.25-8.84%, while the treatment time ranged from 103.5-253.0 s, respectively. In this case, the GW of 30%-70% was found to be most optimized as dose in the heart and lung decreased by up to 4.6% compared to those of the 20%-70% GW and increased by up to 3.0% compared to those of the 40%-60% GW. However, the treatment time when using the 30%-70% GW was 24 s longer than using the 20%-70% GW but 95 s shorter than using 40%-60% GW.

Conclusion: Respiratory gating led to a reduction of the target volume and dose in surrounding normal tissues. A trade-off between the increased dose in the OARs and the shorter treatment time needed to be justified for determination of the optimal gating window.

Keywords: Proton therapy, respiratory gating, pencil beam scanning, gating window, treatment time

บทคัดย่อ

หลักการและเหตุผล: การฉายอนุภาคโปรตอนด้วยเทคนิคการสแกนลำรังสีขนาดเล็กช่วยกระจายปริมาณรังสีให้เหมาะสมกับก้อนมะเร็ง โดยอวัยวะปกติได้รับปริมาณรังสีต่ำ ซึ่งส่งผลดีต่อการรักษามะเร็งปอด แต่ก้อนมะเร็ง

และอวัยวะในทรวงอกเคลื่อนไหวตามการหายใจ ทำให้ปริมาณรังสีคลาดเคลื่อนจากแผนการรักษา
วัตถุประสงค์: เพื่อศึกษาประสิทธิภาพของการฉายอนุภาคโปรตอนด้วยเทคนิคการสแกนลำรังสีขนาดเล็กร่วมกับการฉายรังสีตามจังหวะการหายใจ สำหรับช่วงการฉายรังสีขนาดต่าง ๆ ในผู้ป่วยมะเร็งปอดที่มีการเคลื่อนไหวของก้อนมะเร็งมากกว่า 10 มิลลิเมตร โดยคำนึงถึงปริมาณรังสีในอวัยวะปกติและเวลาที่ใช้ในการรักษา
วัสดุและวิธีการ: ภาพเอกซเรย์คอมพิวเตอร์ 4 มิติของผู้ป่วยมะเร็งปอดที่มีการเคลื่อนที่ของก้อนมะเร็ง 11.6 มิลลิเมตร ถูกนำมาใช้ในการศึกษานี้ ผู้วิจัยใช้เทคนิคการกำหนดตำแหน่งของภาพโดยการเปลี่ยนรูปเพื่อหาระยะทางที่ก้อนมะเร็งเคลื่อนที่ในแต่ละช่วงการหายใจเทียบกับช่วงหายใจออก รวมทั้งศึกษาความสัมพันธ์ระหว่างการเคลื่อนที่ของก้อนมะเร็งกับสัญญาณ RPMTM (Real-time-Position-Management) ที่ติดภายนอกร่างกายผู้ป่วย จากนั้นคำนวณแผนการรักษาสำหรับช่วงการฉายรังสีขนาดต่าง ๆ โดยใช้ระบบวางแผนการรักษา matRad เปรียบเทียบตัวแปรเชิงรังสีคณิตในอวัยวะปกติและเวลาที่ใช้ในการรักษาคำนวณโดยใช้ข้อมูลของเครื่อง Varian's ProBeam ระหว่างแผนการรักษาที่มีการติดตามจังหวะการหายใจและไม่มีการติดตามจังหวะการหายใจ
ผลการศึกษา: การเปิดช่วงการฉายรังสีที่ 10%-80%, 20%-70%, 30%-70% และ 40%-60% สามารถลด Dmean ในหัวใจได้ 1.43-14.29% และ Dmeanในปอดได้ 2.25-8.84% โดยใช้เวลาในการรักษา 103.5-253.0 วินาที ตามลำดับ ในกรณีศึกษานี้พบว่า 30%-70% เป็นขนาดของช่วงการฉายรังสีที่เหมาะสม เนื่องจากปริมาณรังสีในหัวใจและปอดลดลงได้สูงสุด 4.6% เมื่อเทียบกับช่วงการฉายรังสี 20%-70% และเพิ่มขึ้นได้สูงสุด 3.0% เมื่อเทียบกับช่วงการฉายรังสี 40%-60% ในขณะเดียวกันเวลาที่ใช้การรักษาเพิ่มขึ้นเพียง 24 วินาที เมื่อเทียบกับช่วงการฉายรังสี 20%-70% แต่ลดลงถึง 95 วินาที เมื่อเทียบกับช่วงการฉายรังสี 40%-60%
ข้อสรุป: ช่วงการฉายรังสีที่มีขนาดลดลงทำให้ปริมาตรเป้าหมายและปริมาณรังสีในอวัยวะปกติลดลง แต่เพิ่มเวลาที่ใช้ในการรักษา การประเมินขนาดของช่วงการฉายรังสีที่เหมาะสมจะต้องเปรียบเทียบระหว่างปริมาณรังสีในอวัยวะปกติและเวลาที่ใช้ในการรักษา
คำสำคัญ: การฉายอนุภาคโปรตอน, การฉายรังสีตามจังหวะการหายใจ, การสแกนลำรังสีขนาดเล็ก, ขนาดช่วงการฉายรังสีต่อรอบการหายใจ, เวลาที่ใช้ในการรักษา

J Thai Assoc Radiat Oncol 2021; 27(2): R60-R75

Introduction

Proton therapy (PT) has become of increasing interest because of the finite range of proton beams, resulting in decreased dose to surrounding normal tissues compared to photon therapy. The most advanced delivery technique in PT is the pencil beam scanning (PBS) technique, which has better capability of delivering conformal dose to the target with a relatively low dose to normal tissues compared to the passive scattering technique[1]. Several studies have shown the advantage of PBS for lung cancer treatment in term of sparing the nearby healthy organs such as the lung and heart[2-5]. However, the main challenge of the treatment in the chest region is the moving target, especially the movement due

to the respiratory system. The misplacement of spots due to respiratory tumor motion during dynamic beam delivery with PBS, the so-called "interplay effect"[2], can result in severe underdosing in the target and overdosing in surrounding normal tissues and, thus, reducing the effectiveness of the treatment[6]. Many mitigation techniques have been proposed to reduce the interplay effect such as breath-hold, abdominal compression, rescanning and gating techniques. In general, rescanning and gating techniques allow the patient to breathe freely during the treatment with more patient comfort compared to breath-hold and abdominal compression techniques. In the past decade, several research groups have demonstrated that the rescanning technique can potentially reduce the interplay effect[7] but it is still a challenge in the target with a large motion[8-10]. To overcome this obstacle, the combination of rescanning and gating is a promising approach leading to a reduction of the target volume, namely, the internal target volume (ITV)[11, 12]. However, the optimal gating window (GW) to be combined with the rescanning technique is still unclear due to the trade-off between normal tissue sparing and the treatment time.

The objective of this pilot work was to investigate the efficiency of choosing different GWs for treating a lung cancer patient with a target motion of larger than 10 mm using PBS proton therapy in terms of dosimetry for organs at risk (OARs) and treatment time. The GW was defined using the relationship between external and internal motion based on a four-dimensional computed tomography (4DCT) dataset. The treatment plans were created with various GWs and then the dosimetric parameters and the treatment time were investigated for each scenario.

Materials and methods

A. Patient and image dataset

A lung cancer patient treated with photon beam at Department of Radiation Oncology, Chulabhorn Hospital was used in this retrospective study. Ethical approval for this study was obtained from Human Research Ethics Committee, Chulabhorn Research Institute (Project Code: 114/2563). The patient was diagnosed with stage III (T3N3M0) lung adenocarcinoma at the lower lobe of the left lung. The patient had the tumor motion with the magnitude of 11.6 mm. The patient information was acquired using the 16-slice Brilliance CT Big Bore 4DCT scanner (Philips Healthcare, Cleveland, OH) integrated with the Real-time Position Management (RPM™) (Varian Medical Systems, Palo Alto, CA) with the scanning protocol described in **Table 1**. The patient's respiratory pattern from the RPM is shown in **Figure 1**. After the data acquisition, image post-processing was performed to reconstruct the 4DCT images in 10 respiratory phases using the phase-based sorting.

B. Delineation of target volumes and OARs

In this study, the average intensity projection (AIP) images of the 4DCT image dataset were used for ungated and gated treatment plans. For a gated plan, the 4DCT images within a selected

Table 1 The scanning parameters used in the 4DCT image acquisition.

Parameters	Value
Slice thickness (mm)	3
Increment (mm)	-3
Voltage (kV)	120
Current (mAs/Slice)	400
Pitch	0.079
Rotation time (s)	0.5
Field of view (mm)	500
Reconstruction filter	Standard (B)

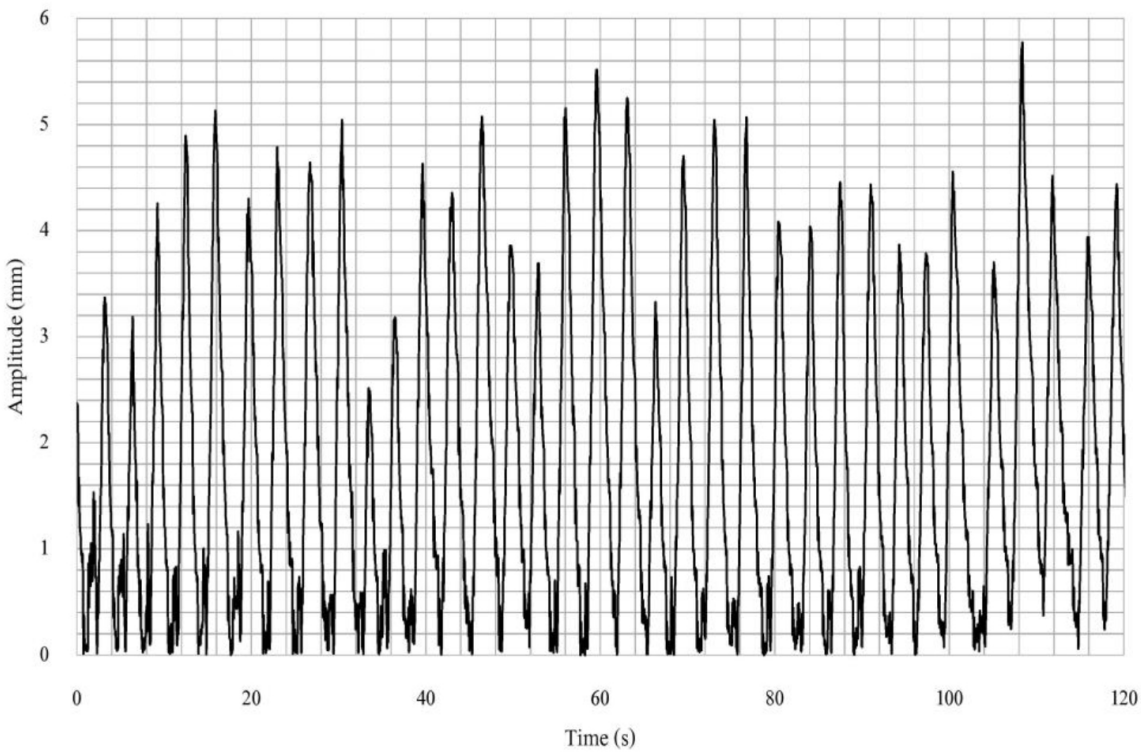


Figure 1 The patient's respiratory pattern with end exhalation as the reference.

GW were used to create the AIP images specific to that GW. For each GW, the target was delineated by a single expert radiation oncologist. The clinical target volume (CTV) was created by extending the gross target volume (GTV) with the margin of 8 mm[13], while the internal clinical target volume (iCTV) was created to encompass the CTVs in selected phases and then the planning target volume (PTV) was obtained by adding the geometrical margin of 5 mm to the iCTV. **Figure 2** illustrates of how iCTV and PTV were generated for each GW. The OARs from the initial photon plan, including esophagus, heart, lung and spinal cord, were transferred by using deformable registration and reviewed by the radiation oncologist. These OAR contours were used for all GWs.

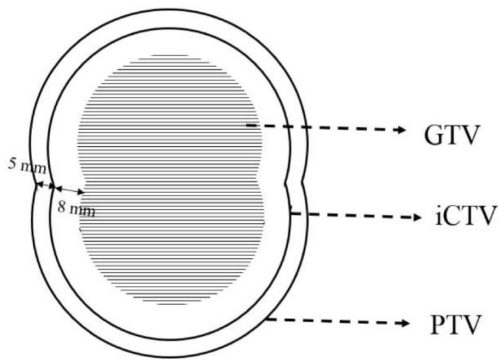


Figure 2 Illustration of iCTV and PTV generation for each gating window.

C. Gating window selection

The GW corresponded to the internal motion of the GTV that covered the selected respiratory phases. In this study, the internal motion of the GTV was related to the RPM signal, which was used to identify the respiratory phases. The external motion was defined as the amplitude of the RPM signal taken for all phases during the image acquisition from the surrogate box placed on the xiphoid position and moving in the anterior-posterior direction. The internal target motion was obtained by deforming the GTV in each phase to the end-exhalation phase (50%) using the deformable image registration algorithm of RayStation version 8B (RaySearch, Stockholm, Sweden). The internal motion was defined as the distance in a three-dimensional space between the centroid of the deformed GTV at a specific phase to that of the non-deformed GTV at 50% phase. The relationship between the internal target motion and the external surface motion was calculated using the linear regression fit.

D. Treatment planning

The PBS proton therapy plans were created with matRad[14], an open-source multi-modality radiation treatment planning system based on generic treatment machines. In the database of matRad, the therapeutic proton beam energies range from 31.7 MeV to 236.1 MeV. The isocenter of the treatment beam was automatically placed at the center of the GTV. The spot size available in the generic machine dataset of matRad was 5 mm. Two beams were applied with the gantry angles of 80° and 170°. In this study, the spot spacing was set to 4 mm. The PTV was prescribed with the relative biological effectiveness (RBE)-weighted dose of 60 Gy(RBE) in 20 fractions. The control condition was that $D_{98\%}$ of the PTV was equal to 95% of the prescribed dose, namely, 57 Gy(RBE). The treatment planning was based on the squared dose deviation objective for the target and the OAR dose constraints were set following the clinical guideline at Chulabhorn Hospital modified by dosimetric compliance criteria for normal tissue[15, 16] as shown in **Table 2**.

The treatment plans from matRad provided the weight, or the number of protons, for each PBS spot. The energies of protons required for the treatment plan calculated in this study were from 52.2 to 135.1 MeV. Since matRad was developed for a generic machine, the conversion from spot weights to monitor units (MU) was assumedly taken from the machine-specific beam data of ProBeam (Varian Medical Systems, Palo Alto, CA), which are available for 70-240 MeV proton energies[17]. For protons with energies lower than 70 MeV, the conversion factors were extrapolated with the spline function in MATLAB. According to Poulsen et al[18], the minimum MU (MU_{min}) of ProBeam was 1.1. In this work, the spots with the MUs less than 1.1 were removed from the treatment plans. The numbers of spots before and after spot elimination for each plan are shown in **Table 3**.

Table 2 The OAR dose constraints following the clinically used guideline at Chulabhorn Hospital modified from dosimetric compliance criteria for normal tissue[15, 16].

Organs	Dose constraints		
Esophagus	$D_{mean} \leq 34$ Gy	No hot spot	
Heart	$D_{mean} \leq 26$ Gy	$D_{50\%} \leq 30$ Gy	$D_{46\%} \leq 30$ Gy
Each lung	$D_{mean} \leq 20$ Gy	$V_{5Gy} \leq 65\%$	$V_{20Gy} \leq 30\%$
Spinal cord	$D_{2\%} \leq 45$ Gy		

Table 3 The number of scanning spots in the original plans and the new plan after eliminating spots with MU lower than 1.1.

Treatment plans (GWs)	Number of scanning spots					
	Original plans			New plans		
	80°	170°	Total	80°	170°	Total
Ungated	2657	2703	5360	1642	1695	3337
10% - 80%	2400	2419	4819	1545	1607	3152
20% - 70%	2184	2218	4402	1305	1423	2728
30% - 70%	2136	2168	4304	1378	1443	2821
40% - 60%	1950	1985	3935	1295	1340	2635

Therefore, to be able to compare the treatment plans for the different GWs, each plan was normalized so that $D_{98\%}$ of the PTV was equal to 57 Gy(RBE) ($D_{98\%}$ = 95%). **Figure 3** shows the dose distribution and beam orientation of each treatment plan on the AIP image of the 4DCT dataset specific to each GW. The following dosimetric parameters were compared between the treatment plans with different GWs by using the ungated treatment plan as the reference: D_{mean} for esophagus, heart and lung; $D_{2\%}$ for spinal cord; and V_{5Gy} and V_{20Gy} for lung.

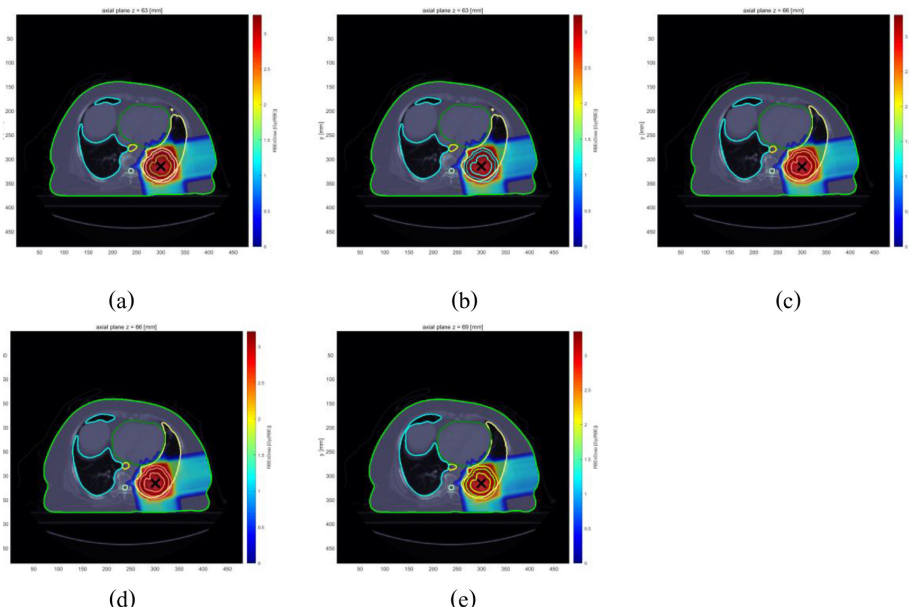


Figure 3 Dose distributions (Gy(RBE)) and beam orientation (80° and 170°) on the average intensity projection images of the 4DCT datasets of the ungated and gated plans: (a) ungated, (b) 10% - 80% GW, (c) 20% - 70% GW, (d) 30% - 70% GW, and (e) 40% - 60% GW.

E. Treatment time evaluation

To calculate the treatment time for the ungated treatment plan, published information related to the beam delivery time of a ProBeam machine was used. Following Poulsen et al[18], three parameters consisting of energy switching time (t_{switch}), waiting time (t_{wait}) and beam-on time ($t_{beam\text{-}on}$) were required for the determination of the ungated treatment time as follows

$$t_{\text{ungated}} = t_{\text{switch}} + t_{\text{wait}} + t_{\text{beam-on}} \quad (1)$$

The detail of equation (1) is given in the Appendix.

For the gated treatment plans, the patient's breathing cycle period from the RPM signal with 34 cycles was averaged to 3.4 s/cycle. This patient's breathing cycle was divided equally into 10 respiratory phases with 0.34 s/phase. The breathing cycle period and the ungated treatment time were used to predict the number of breathing cycles required for completing the treatment and to calculate the total treatment time with the gating technique for the different GWs (tgated,GW), as follows

$$t_{\text{gated,GW}} = \left(\left\lceil \frac{t_{\text{ungated}}}{t_{\text{GW}}} \right\rceil \times 3.4 \text{ s/cycle}\right) - \left[t_{\text{GW}} - \text{mod}\left(\frac{t_{\text{ungated}}}{t_{\text{GW}}}\right)\right] - t_{\text{surplus}} \quad (2)$$

where t_{GW} is the time duration of the GW calculated by

$$t_{\text{GW}} = N_{\text{GW}} \times 0.34 \text{ s/phase} \quad (3)$$

N_{GW} is the number of phases in the GW per breathing cycle. The function $\left\lceil \frac{t_{\text{ungated}}}{t_{\text{GW}}} \right\rceil$ in equation (2) yields the ceiling of the division, obtained by rounding up the division to the nearest integer, with the value of this function corresponding to the number of required breathing cycles for the beam delivery. The function "mod" is the modulo function, giving the remainder of the division. $t_{surplus}$ is the time difference between the end of the breathing cycle and the end of the GW. It is to note that for simplicity it was assumed that the beam delivery always started at the beginning of the GW.

Results

Figure 4 shows the linear relationship between the internal target motion and the external surface motion with the coefficient of determination (R^2) from the linear regression fit of 0.9731. This means that in this case the external motion could be used to identify the respiratory motion of the target.

Table 4 shows the relationship of internal motions, external motions and coverages of respiratory phases for the investigated case. In this study, five values of the tumor motions ranging from ≤1.4 to ≤11.6 mm were manually selected for the investigation, corresponding to the external motions ranging from ≤0.4 to ≤4.0 mm, and the GWs of 40% - 60%, 30% - 70%, 20% - 70%, 10% - 80% and 10%-90% (ungated), respectively.

Table 5 shows the PTV volumes for the selected GWs. The PTV volume increased as the GW was increased. The treatment plans for all investigated GWs passed the criteria of dose constraints as listed in **Table 2**. **Table 6** gives the

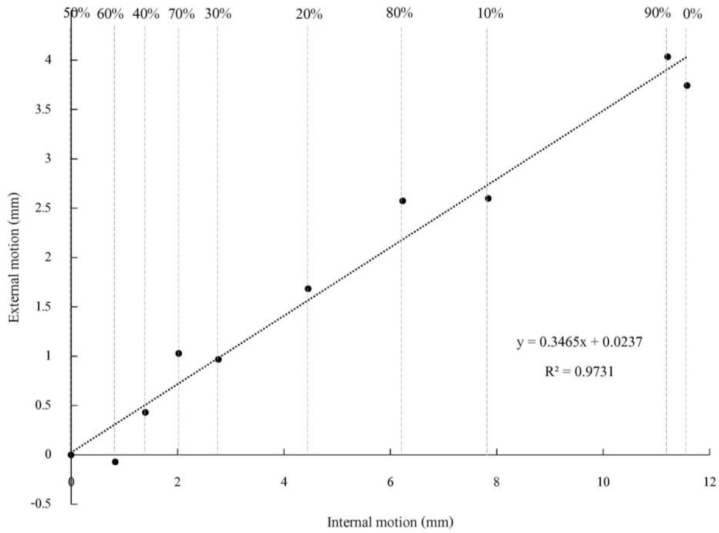


Figure 4 The relationship between external and internal motions used for gating window selection in the investigated case. The symbols are the measured data and the line is the fitted linear curve. The vertical dashed lines represent the respiratory phases of this patient.

resulting dosimetric parameters of the PTV and OARs for all treatment plans and **Figure 5** illustrates the percentage differences of the dosimetric parameters of the OARs for the different GWs relative to the ungated plan. From **Figure 5** it was found that the dosimetric parameters for these OARs were reduced with the narrower GW except for the esophagus, for which D_{mean} for the 40%-60% GW was about 10% higher than that for the 30%-70% GW. The reduced GW resulted in dose reduction in the OARs by up to 14.3% for D_{mean} in the heart, 8.8% for D_{mean} in the left lung, 8.8% for Dmean in the total lung, 5.5% for V_{5Gy} in the left lung, 5.5% for V_{5Gy} in the total lung, 7.6% for V_{20Gy} in the left lung, and 7.7% for V_{20Gy} in the total lung.

Table 4 The relationship of internal motions, external motions and coverages of respiratory phases for the investigated case.

Internal motion (mm)	External motion (mm)	Gating window (Respiratory phase coverage)
≤1.4	≤0.4	40% - 60%
≤2.8	≤1.0	30% - 70%
≤4.5	≤1.7	20% - 70%
≤7.8	≤2.6	10% - 80%
≤11.6 (Ungated)	≤4.0 (Ungated)	0% - 90%

Table 5 PTV volume and treatment time for the different gating windows.

Gating window	PTV volume (cm^3)	Treatment time (s)
Ungated	216.1	89.5
10%-80%	200.4	103.5
20%-70%	186.8	133.8
30%-70%	181.8	158.2
40%-60%	170.0	253.0

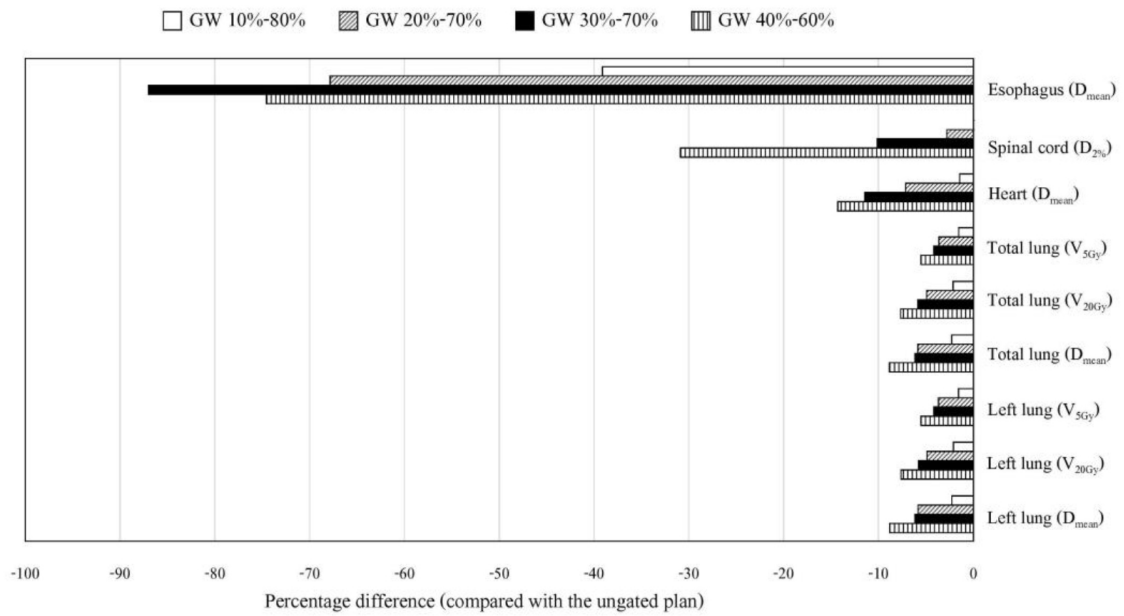


Figure 5 Percentage differences of D_{mean}, $D_{2\%}$ and D_{mean} for esophagus, spinal cord and heart. V_{5Gy}, V_{20Gy} and D_{mean} for the total lung and the left lung compared to the ungated treatment plan, respectively. The percentage differences were calculated from $(D_{plan} - D_{ungated\ plan}) / D_{ungated\ plan} \times 100$.

Table 5 shows the total treatment time for each GW. It was found that the treatment time increased as the GW was decreased. The percentage differences of the treatment time using the ungated plan as the reference were 15.6%, 49.5%, 76.8%, and 182.7% for the 10%-80%, 20%-70%, 30%-70% and 40%-60% GWs, respectively.

Table 6 Dosimetric parameters of the PTV and OARs for each treatment plan. These values were rounded to 2 decimal places.

Dosimetric parameters (Gy(RBE) or % volume)		Gating window				
		Ungated	10% - 80%	20% - 70%	30% - 70%	40% - 60%
PTV[a]	$D_{98\%}$	57	57	57	57	57
Esophagus	D_{mean}	4.66×10^{-7}	2.84×10^{-7}	1.50×10^{-7}	6.07×10^{-8}	$1.19\times1^{0-7}$
Spinal cord	$D_{2\%}$	0.79	0.79	0.77	0.71	0.55
Heart	D_{mean}	0.14	0.14	0.13	0.12	0.12
	$D_{50\%}$	0	0	0	0	0
Total lung	D_{mean}	7.06	6.90	6.65	6.63	6.44
	V_{5Gy}	14.90%	14.67%	14.36%	14.28%	14.08%
	V_{20Gy}	13.19%	12.91%	12.54%	12.42%	12.18%
Left lung	D_{mean}	16.42	16.05	15.46	15.41	14.97
	V_{5Gy}	34.67%	34.13%	33.40%	33.23%	32.76%
	V_{20Gy}	30.67%	30.03%	29.17%	28.90%	28.33%

[a]Each plan was normalized so that $D_{98\%}$ of the PTV was equal to 57 Gy(RBE) ($D_{98\%}$ = 95%).

Discussion

In general, the narrower GW yielded smaller treated volumes. Similarly, the study of Jang et al.[19] showed that the ITV reduction and smaller D_{mean} in the normal lung could be achieved by gated photon therapy. In this work, some exceptions were observed in the investigated case. From **Figure 5,** it can be seen that esophagus received about 10% higher dose for the GW of 40%-60% compared to the 30%-70% GW. However, esophagus dose was very low, i.e. the absolute dose was 6.1×10^{-8} Gy(RBE) for the 30%-70% GW and 1.2×10^{-7} Gy(RBE) for the 40%-60% GW, and, in this case, not clinically relevant. Therefore, the difference in esophagus doses made no contribution to the selection of the optimal GW.

In this study, the GW of 30%-70% was found to be most optimized for the following reasons. By using the 30%-70% GW, the dosimetric parameters in the heart and lung were reduced by up to 4.6% compared to those of the

20%-70% GW and increased by up to 3.0% compared to those of the 40%-60% GW. In addition, the treatment time when using the 30%-70% GW was 24 s longer than using the 20%-70% GW but 95 s shorter than using 40%-60% GW. In this case, a trade-off between the increased dose in the OARs and the shorter treatment time for the 30%-70% GW compared with the 40%-60% GW needed to be justified. Since all treatment plans actually passed the criteria of dose constraints for the OARs, but the longer treatment time would cause more patient movement. Therefore, the optimal GW in this case was chosen to be 30%-70%, which corresponded to ≤2.8 mm internal motion.

Some limitations of the present work should be noted. First, this study included only one patient due to the limited number of available cases that underwent 4DCT image acquisition and showed a large tumor motion (≥10 mm). The correlation of external and internal motion could be different in other cases. However, the strong linear relationship of external and internal motion shown in this study agreed with the result of Zhang et al[20] and Liu et al[21]. Second, since matRad was developed based on generic treatment machines, the evaluation of MUs and treatment time could only be done by employing available machine-specific data such as those obtained from the literature for the ProBeam machine[18]. The actual treatment time with ProBeam for the same scenarios could be different from those reported here especially when using different optimizers. However, the trend of the treatment time with the GW obtained in this work should comply with actual situations. It is to note that a combination of rescanning and gating has been proposed for treatment of moving targets. In that case, the treatment time could be increased by. 2-3 times with layered rescanning and more than 8 times with volumetric rescanning compared to gating without rescanning[20]. Lastly, it was not possible to set the minimum MU during the optimization process in matRad. Therefore, manual subtraction of spots with the MU less than a specified cut-off value (in this case, 1.1 MU) was carried out. If the treatment planning system could consider the minimum MU, the treatment plan could be different than those obtained here. Nevertheless, we have confirmed that after removing the low MU spots and normalizing $D_{98\%}$ of the PTV to 95% of the prescribed dose (57 Gy(RBE)), the target dose coverage and the dose constraints at OARs could still be achieved. Therefore, the removal of low MU spots as done in this study was acceptable.

In this study, the open-source treatment planning toolkit matRad was used for calculating the proton dose distribution. MatRad uses the pencil beam algorithm for dose calculation and has been validated against the clinically used Syngo RT Planning[14]. The limitation of the pencil beam algorithm for heterogeneous lung tissues are well known and a Monte Carlo dose engine should be used for the clinical treatment planning of lung cancer[22]. However, in this work we focused on the effect of the different gating windows on OAR doses and treatment time in a comparative manner. Therefore, the choice of

the dose calculation algorithm should not affect the overall validity of the conclusions.

Conclusion

This paper describes a pilot study to investigate the influence of the gating window on dosimetric parameters and treatment time in PBS proton therapy for lung cancer with a large target motion (≥10 mm). The gating technique reduced the target volume, meaning that normal tissues received smaller dose with the smaller gating window. Conversely, by reducing the gating window, the beam-on time in a breathing cycle was decreased and subsequently the treatment time was increased. The selection of the gating window should be optimized between sparing normal tissues and reasonable treatment time. In this case, the optimal gating window was found to be 30%-70%. The result of this work will be used in the study of the efficiency of the combined gating and rescanning technique in PBS proton therapy for lung cancer.

Acknowledgments

The authors declare that there is no conflict of interest.

Appendix

Following Poulsen et al[18], the ungated treatment time was calculated with equation (1), depending on energy switching time (t_{switch}), waiting time (t_{wait}) and beam-on time ($t_{beam\text{-}on}$). In this study, t_{switch} was set to 0.9 s[23]. twait is the time duration used for changing the scanning spot. If the distance between two consecutive spots was 10 mm or more than 10 mm ($d_{threshold}$), the beam was assumed to be turned off before going to the next spot[18]. t_{wait} was defined as

$$t_{\text{wait}} = \begin{cases} 0, \ \text{if } \Delta x < d_{\text{threshold}} \text{ and } \Delta y < d_{\text{threshold}} \\ \max\left(t_{0,x} + \dfrac{\Delta x}{v_{\text{x}}}, t_{0,y} + \dfrac{\Delta y}{v_y} \right), \text{otherwise} \end{cases} \quad \text{(A 1)}$$

$t_{0,x}$ and $t_{0,y}$ are the values of delayed time in the x-axis and the y-axis, corresponding to 2.85 and 3.52 ms, respectively[18]. The scanning speed in the x-axis (v_x) and the y-axis (v_y) were set to 6.92 and 32.1 mm/ms, respectively[18]. "Δx" and "Δy" are the distances between spots in x-axis and y-axis, respectively. Originally, the spot spacing was set to 4 mm, requiring no waiting time. However, since the spots with the MUs lower than 1.1 were removed from the plans, the distances between some consecutive spots were larger than 10 mm.

$t_{beam\text{-}on}$ is the time duration for delivering the dose to each spot until achieving the MU required by the treatment plan, defined as

$$t_{\text{beam-on}} = MU \cdot \left(\frac{t_{\min}}{MU_{\text{min_layer}}} \right) \quad \text{(A 2)}$$

$$t_{\min} = \begin{cases} 1.94 \text{ ms, if } MU_{\text{min_layer}} > MU_{\min} \\ 1.62 \text{ ms, if } MU_{\text{min_layer}} = MU_{\min} \text{ and energy} > 149 \text{ MeV} \\ 2.13 \text{ ms, if } MU_{\text{min_layer}} = MU_{\min} \text{ and energy} < 149 \text{ MeV} \end{cases} \quad \text{(A 3)}$$

where MU is the monitor unit of the scanning spot, MU_{min_layer} is the lowest MU in the same energy layer and t_{min} is the shortest beam-on time in the same energy layer given by equation (A 3).

References

1. Paganetti H, Bortfeld T. Proton Therapy. In: Schlegel W, Bortfeld T, Grosu A-L, editors. New Technologies in Radiation Oncology. Berlin, Heidelberg: Springer Berlin Heidelberg; 2006. p. 345-63.
2. Han Y. Current status of proton therapy techniques for lung cancer. Radiat Oncol J. 2019;37:232-48.
3. Chang JY, Zhang X, Wang X, Kang Y, Riley B, Bilton S, et al. Significant reduction of normal tissue dose by proton radiotherapy compared with three-dimensional conformal or intensity-modulated radiation therapy in Stage I or Stage III non–small-cell lung cancer. Int J Radiat Oncol Biol Phys. 2006;65:1087-96.
4. Nichols RC, Huh SN, Henderson RH, Mendenhall NP, Flampouri S, Li Z, et al. Proton radiation therapy offers reduced normal lung and bone marrow exposure for patients receiving dose-escalated radiation therapy for unresectable stage III non-small-cell lung cancer: a dosimetric study. Clin Lung Cancer. 2011;12:252-7.
5. Oh D. Proton therapy: the current status of the clinical evidences. Precis Future Med. 2019;3:91-102.
6. Bert C, Durante M. Motion in radiotherapy: particle therapy. Phys Med Biol. 2011;56:R113.
7. Phillips MH, Pedroni E, Blattmann H, Boehringer T, Coray A, Scheib S. Effects of respiratory motion on dose uniformity with a charged particle scanning method. Phys Med Biol. 1992;37:223.
8. Seco J, Robertson D, Trofimov A, Paganetti H. Breathing interplay effects during proton beam scanning: simulation and statistical analysis. Phys Med Biol. 2009;54:N283.
9. Zhang Y, Huth I, Wegner M, Weber DC, Lomax AJ. An evaluation of rescanning technique for liver tumour treatments using a commercial PBS proton therapy system. Radiother Oncol. 2016;121:281-7.
10. Engwall E, Glimelius L, Hynning E. Effectiveness of different rescanning techniques for scanned proton radiotherapy in lung cancer patients. Phys Med Biol. 2018;63:095006.
11. Underberg RW, Lagerwaard FJ, Slotman BJ, Cuijpers JP, Senan S. Benefit of respiration-gated stereotactic radiotherapy for stage I lung cancer: an analysis of 4DCT datasets. Int J Radiat Oncol Biol Phys. 2005;62:554-60.
12. Giraud P, Morvan E, Claude L, Mornex F, Le Pechoux C, Bachaud J-M, et al. Respiratory gating techniques for optimization of lung cancer radiotherapy. J Thorac Oncol. 2011;6:2058-68.
13. Giraud P, Antoine M, Larrouy A, Milleron B, Callard P, De Rycke Y, et al. Evaluation of microscopic tumor extension in non–small-cell lung cancer for three-

dimensional conformal radiotherapy planning. Int J Radiat Oncol Biol Phys. 2000;48:1015-24.
14. Wieser HP, Cisternas E, Wahl N, Ulrich S, Stadler A, Mescher H, et al. Development of the open-source dose calculation and optimization toolkit matRad. Med phys. 2017;44:2556-68.
15. Giaddui T, Chen W, Yu J, Lin L, Simone CB, Yuan L, et al. Establishing the feasibility of the dosimetric compliance criteria of RTOG 1308: phase III randomized trial comparing overall survival after photon versus proton radiochemotherapy for inoperable stage II-IIIB NSCLC. Radiat Oncol. 2016;11:1-7.
16. Marks LB, Yorke ED, Jackson A, Ten Haken RK, Constine LS, Eisbruch A, et al. Use of normal tissue complication probability models in the clinic. Int J Radiat Oncol Biol Phys 2010;76:S10-9.
17. Rahman M, Bruza P, Lin Y, Gladstone DJ, Pogue BW, Zhang R. Producing a Beam Model of the Varian ProBeam Proton Therapy System using TOPAS Monte Carlo Toolkit. Med Phys. 2020;47:6500-08.
18. Poulsen PR, Eley J, Langner U, Simone II CB, Langen K. Efficient interplay effect mitigation for proton pencil beam scanning by spot-adapted layered repainting evenly spread out over the full breathing cycle. Int J Radiat Oncol Biol Phys. 2018;100:226-34.
19. Jang SS, Huh GJ, Park SY, Yang PS, Cho EY. The impact of respiratory gating on lung dosimetry in stereotactic body radiotherapy for lung cancer. Phys Med. 2014;30:682-9.
20. Zhang Y, Huth I, Wegner M, Weber DC, Lomax AJ. Surface as a motion surrogate for gated re-scanned pencil beam proton therapy. Phys Med Biol. 2017;62:4046.
21. Liu C, Alessio AM, Kinahan PE. Respiratory motion correction for quantitative PET/CT using all detected events with internal—external motion correlation. Med Phys. 2011;38:2715-23.
22. Winter J, Ellerbrock M, Jäkel O, Greilich S, Bangert M. Analytical modeling of depth-dose degradation in heterogeneous lung tissue for intensity-modulated proton therapy planning. Phys and Im in Rad Onc. 2020;14:32-8.
23. Langner UW, Eley JG, Dong L, Langen K. Comparison of multi-institutional Varian ProBeam pencil beam scanning proton beam commissioning data. J Appl Clin Med Phys. 2017;18:96-107.